

Customised Mode Profiles Using Functional Materials

Jonathan Gratus^{1,2,*}, Paul Kinsler^{1,2,†}, Rosa Letizia^{1,3}, and Taylor Boyd^{1,2}

¹Cockcroft Institute, Keckwick Lane, Daresbury, WA4 4AD, United Kingdom.

²Physics Department, Lancaster University, Lancaster LA1 4YB, United Kingdom. and

³Engineering Department, Lancaster University, Lancaster LA1 4YW, United Kingdom.

(Dated: Monday 18th July, 2016)

We show how to control the field profile on a sub-wavelength scale using a customised permittivity variation in a functional medium, thus avoiding the need to e.g. synthesize the shape from its Fourier harmonics. For applications such as beam dynamics, requiring field profile shaping in free space, we show that it is possible to achieve this despite using a slot in the medium.

We show how we can use layered or varying material properties to sculpt the electric field profile along the propagation direction. Here we use *sub-wavelength* variation as a means of controlling the internal field profile [1, 2], in contrast to the typical uses of layered [3] or chirped [4] 1D photonic crystals, whose focus is primarily on manipulating the band structure, reflectivity, or transmission properties. Up to now most of the work has concentrated on photonic band gaps in photonic crystals, and the transmission or reflection coefficients at various angles or frequencies of an incident wave [5]. Our method is also distinct from the synthesis of optical waveforms by combining carefully phased harmonics [6, 7].

Many possibilities are unlocked by our ability to design field profiles with sub-wavelength customization. We might imagine enhancing ionization in high harmonic generation (HHG, see e.g. [8] and citations thereof), where the field profile aims to give a detailed control of the ionized electrons trajectory and recollision. Further, we might create localized peaks in the waveform, so that the concentration of optical power enhances the signal to noise ratio, or gives a larger nonlinear effect. Conversely, flatter profiles could help minimise unwanted nonlinear effects, or better localise the sign transition as happens for a square wave signal. In accelerator applications, there is much interest in controlling the size and/or shape of electron bunches (see e.g. [9]), or for pre-injection plasma ionisation for laser wakefield acceleration [10]; sculpted electric field profiles are one way of achieving the desired level of control.

Of course, when using customised field profiles to control an electron bunch in an accelerator or synchrotron, we need that field profile to be present in free space. We address this important case using a gap between two slabs of the necessary customised medium, and use CST Studio Suite [11] simulations of this arrangement to demonstrate that the desired field profile is still present within the slot. A slot also enables probes to be placed to measure the electric field, and can increase the transmission of external fields into the medium.

To motivate our scheme we first consider assuming (or guessing) some promising dielectric function $\epsilon(z)$, and solving the wave equation for $\mathbf{E}(z)$ under those conditions, and varying the parameters to search for a suitable field profile.

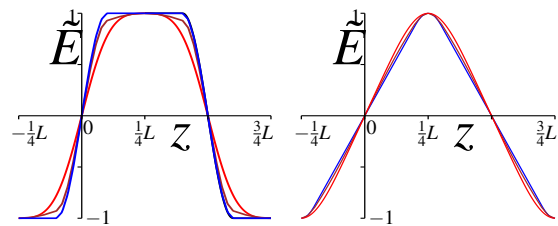


FIG. 1: Left: Field profiles for the ‘flat-top’ structure with $\epsilon(z)$ as defined in (5), where $\ell = L/10$. Right: Field profiles for the ‘triangular’ structure with $\epsilon(z)$ as defined in (6), where $\ell = L/10$. In both cases we have not plotted the predicted field as it is coincident (at this resolution) to the simulated CST simulated field profile for \tilde{E}_x (blue). The brown curve is the CST generated field profile *in the slot*, when a slot of $\frac{1}{6}$ (flat-top) and $\frac{1}{3}$ (triangular) width is cut in the structure; a good match is still achieved demonstrating that our scheme can also be used to control free-space field profiles. For comparison the Mathieu functions for $n = 1$, and $q = 0.8$ (flat-top) or $q = -0.329$ (triangular) are plotted (red).

By selecting a simple material variation we could make use of existing solutions; notably repeating two-layer structure would allow us to repurpose work on (e.g.) Bragg reflectors. More interesting would be to assume a sinusoidal variation in permittivity, which has a wave equation that matches that for Mathieu functions¹ [12, 13]. The periodic Mathieu functions depend on two parameters a_n, q , where $a_n = a_n(q)$ is the n -th characteristic value. These give solutions of the differential equation for $A_{n,q}(z)$

$$\partial_z^2 A_{n,q}(z) - [a_n - 2q \cos(4\pi z/L)] A_{n,q}(z) = 0. \quad (1)$$

Sample Mathieu functions, with parameters chosen to give both flat-topped and triangular profiles are shown compared to other similar (but explicitly designed) profiles on fig. 1.

However, although Mathieu functions and the like are powerful sources of inspiration, we prefer to follow a design-lead scheme where we first specify the desired field profile $\mathbf{E}(z)$, then use the wave equation to calculate what the position dependent dielectric properties $\epsilon(z)$ needs to be. In principle this allows us to directly calculate the material function needed to support almost any electric field profile we might want.

*Electronic address: j.gratus@lancaster.ac.uk

†Electronic address: dr.paul.kinsler@physics.org

¹ See e.g. <http://mathworld.wolfram.com/MathieuFunction.html>

Consider the single frequency transverse mode with $\mathbf{E} = e^{i\omega t} \tilde{E}(z)\mathbf{i}$, $\mathbf{P} = e^{i\omega t} \tilde{P}(z)\mathbf{i}$ and $\mathbf{H} = e^{i\omega t} \tilde{H}(z)\mathbf{j}$, together with the permittivity $\epsilon(\omega, z) = \epsilon_0 \epsilon_r(\omega, z)$ and vacuum permeability μ_0 . Then Maxwell's equations, where $\prime = \frac{d}{dz}$, give

$$\tilde{E}'' + \omega^2 c^{-2} \epsilon_r(\omega, z) \tilde{E} = 0, \text{ so that } \epsilon_r(\omega, z) = -\frac{c^2 \tilde{E}''}{\omega^2 \tilde{E}}. \quad (2)$$

In principle almost any electric field profile is possible. However, for some field profiles, the solution in (2) requires the presence of negative permittivities, possibly with a very high absolute value; in others \tilde{E}''/\tilde{E} is undefined.

Further, in order to design a simpler structure for the numerical simulations, we choose our permittivity function so that $\epsilon_r > 0$, and that ϵ_r does not change rapidly. This requires the $\tilde{E}''/\tilde{E} < 0$ and that when $\tilde{E}(z) = 0$ then $\tilde{E}''(z) = 0$, i.e. a point of inflection. To simplify the modelling we restrict ourselves to modes with odd symmetry about $z = 0$ and $z = L/2$ and hence even symmetry about $z = L/4$ where L is the desired wavelength. Thus

$$\tilde{E}(z) = -\tilde{E}(-z) = -\tilde{E}(z + \frac{L}{2}) = \tilde{E}(z + L), \quad (3)$$

$$\text{and } \tilde{E}(\frac{L}{4} - z) = \tilde{E}(\frac{L}{4} + z). \quad (4)$$

Thus it is only necessary to specify $\tilde{E}(z)$ for $0 < z < L/4$. The symmetry requirements imply $\tilde{E}(0) = 0$ and $\tilde{E}'(L/4) = 0$. From (4) & (2) one sees that ϵ_r has period half that of E , and has even symmetry about $z = 0$, i.e. $\epsilon_r(z) = \epsilon_r(-z) = \epsilon_r(z + L/2)$.

It is advantageous for the electric field to be composed of piecewise sections which are either sinusoidal, and hence correspond to constant ϵ_r , or linear, which correspond to $\epsilon_r = 0$.

Following this theoretical design step, we validate our scheme using 3D CST simulations based on a rod-like unit cell oriented along z , with a nearly square cross section in x and y . On the x boundary we set a perfect magnetic conductor (i.e. $\mathbf{H}_{\text{trans}} = 0$), and on the y boundary we have a perfect electric conductor (i.e. $\mathbf{E}_{\text{trans}} = 0$). The z boundary conditions are periodic with a phase shift of 180° . We choose these boundary conditions since if we instead used all periodic conditions, then spurious modes with finite k_y or k_z transverse to the variation (in z) would appear.

In this Letter we confine ourselves to consider only material variation that has a strictly positive-valued permittivity everywhere. In part, this is because materials with negative permittivity are typically strongly dispersive, and so there may be – at the very least – stringent bandwidth limitations. With this constraint, and for some choices of profile, it can be more difficult to construct the permittivity function that supports an electric field with sufficient accuracy.

Nevertheless, by using materials with very low permittivity ϵ (epsilon near zero, ENZ), one can construct profiles which are (e.g.) almost flat for a significant proportion of the mode, or which have near constant gradient – both being shown in fig. 1. These profiles were inspired by Mathieu functions of similar appearance, but as we found, that general appearance does not require the specific sinusoidal ϵ variation needed for the Mathieu functions themselves. In addition, profiles with strongly localised peaks can be achieved by combining two

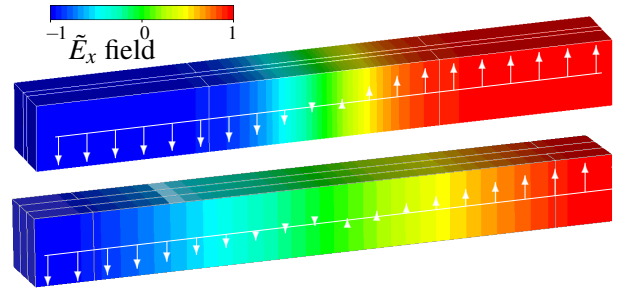


FIG. 2: Results from 3D CST models of the ‘flat-top’ (top) and ‘triangular’ (bottom) wave structure including free-space slots as described in fig. 1, showing the electric field strength and direction through the structure. In both cases the slot field differs from the field in the structure by less than 1%.

materials of significantly different permittivities, and if one is prepared to tolerate less precise profiles, it may be possible to construct reasonable flat-top and triangular profiles using only materials with $\epsilon \geq 1$. For brevity, here we will consider only the four representative profiles indicated in table I.

Shape	Constant ϵ_r	ENZ
Flat	✓	✓
Triangular	✓	✓
Peak with multiple oscillations	✓	✗
Peak with two oscillations	✗	✗

TABLE I: The four electric field profiles considered in this article, and the permittivity properties required to generate them.

FLAT-TOP WAVE PROFILE: A flat-topped, or quasi square-wave profile is a familiar waveform, and is often encountered in digital switching circuits, being naturally of a binary (two-level) form. The fast square-wave transitions are ideal for triggering actions at precisely determined intervals; alternatively its periods of near constant field are ideal for applying a (nearly) identical force to each charged particle in a bunch. However, to synthesize this profile directly from its many harmonic components would require a significant effort, especially if attempting to build an optical square wave (see e.g. [6]). However, using our technique we can sidestep that effort by constructing instead a designer functional material that quite naturally supports such waveforms. We can generate our flat-top wave profile using

$$\tilde{E}(z) = \begin{cases} \sin(\pi z/2\ell), & 0 < z < \ell \\ 1, & \ell < z < \frac{1}{4}L, \end{cases} \quad (5)$$

$$\text{and } \epsilon_r(z) = \begin{cases} c^2 \pi^2 / 4\ell^2 \omega^2, & 0 < z < \ell \\ 0, & \ell < z < \frac{1}{4}L. \end{cases}$$

for ℓ , with $0 < \ell < \frac{1}{4}L$. We implemented this structure in CST, based on a unit cell with cross section $a_x = 6\text{mm}$, $a_y = 6.22\text{mm}$ and length $L = 52\text{mm}$. The slot, when present, was 1mm wide. Fig. 1 demonstrates that the designed-for

field profile is achievable even in a 3D simulation; a 3D visualization is given in fig. 2.

TRIANGULAR WAVE PROFILE: A field profile with a triangular form, just like a square wave or indeed any waveform can be synthesized from its harmonics. In comparison to the square wave in particular, though, the proportion of higher harmonics falls off more rapidly, so any synthesis would in practise be easier. This ramped field profile could also be used to impart a well-managed linear chirp to charged particles in a bunch.

Nevertheless, here we can design a structure which naturally supports triangular waves, which is given by

$$\begin{aligned} \tilde{E}(z) &= \begin{cases} k \sin(k\ell - \frac{1}{4}kL)z, & 0 < z < \ell \\ \cos(kz - \frac{1}{4}kL), & \ell < z < \frac{1}{4}L, \end{cases} \quad (6) \\ \text{and } \epsilon_r(z) &= \begin{cases} 0, & 0 < z < \ell \\ c^2k^2/\omega^2, & \ell < z < \frac{1}{4}L, \end{cases} \end{aligned}$$

where ℓ , with $0 < \ell < \frac{1}{4}L$, and let $k > 0$ be the lowest solution to $\ell k = \cot(\frac{1}{4}Lk - \ell k)$. We implemented this structure in CST, based on the same unit cell as for the flat-top wave; except that when present the slot width was 2mm. Fig. 1 demonstrates that the designed-for field profile is achievable even in a full 3D simulation. A 3D visualization is given in fig. 2.

A saw-tooth profile could be created in a similar manner by using an ENZ material for the linearly increasing section of the wave, and then a relatively high permittivity segment for the short near-vertical connecting part. Such a wave profile was suggested as a ‘gradient gating’ way of optimising HHG [8]; the idea being that the initial strong field could ionize a gas atom and accelerate the electron away, before returning to the nucleus to recombine and emit high-energy photons. Subsequent work has focussed on optimising the field profiles on the basis of detailed models of the ionization process [14]. Given such a wave profile, our method could be used to design a structure to generate it – although tolerating the intense laser pulses used would be a challenge.

PEAKED PROFILE WITH MULTIPLE OSCILLATIONS: Waveforms with strongly localized peaks can also be useful, particularly where an amplitude and/or intensity threshold is the chosen discriminator. However, just like any wave with distinct or localized features, they have a significant harmonic content and we might therefore prefer not to synthesize them directly. Unfortunately, as we have noted, long intervals of a near-constant electric field in a waveform require very small permittivity values (i.e. the ENZ regime). To avoid this complication, we might replace an idealized near-constant region with many low-amplitude rapid oscillations that are assumed to cycle-average to zero.

In the range $0 < z < \ell$ there is a small $\tilde{E}(z)$ with n oscillations, whereas the range $\ell < z < \frac{1}{4}L$ provides the desired single large oscillation. The profile is chosen so that $\tilde{E}(\ell) = 0$,

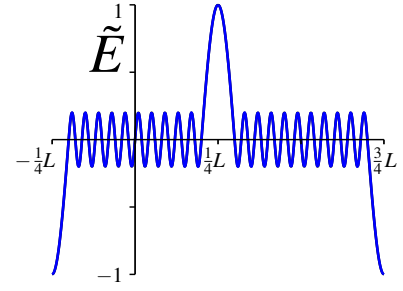


FIG. 3: Field profiles for the the ‘multi-oscillation wave’ structure with $\epsilon(z)$ as defined in (7), $\ell = (0.8)\frac{1}{4}L$ and $n = 5$. The CST simulated field profile for \tilde{E}_x (blue) is nearly coincident with the designed-for profile from (7).

so that

$$\begin{aligned} \tilde{E}(z) &= \begin{cases} \frac{\ell \sin(2n\pi z/\ell)}{4n(\frac{1}{4}L - \ell)}, & 0 < z < \ell \\ \cos\left[\frac{\pi(\frac{1}{4}L - z)}{2(\frac{1}{4}L - \ell)}\right], & \ell < z < \frac{1}{4}L, \end{cases} \quad (7) \\ \text{and } \epsilon_r(z) &= \begin{cases} 4c^2n^2\pi^2/\omega^2\ell^2, & 0 < z < \ell \\ c^2\pi^2/4\omega^2(\frac{1}{4}L - \ell)^2, & \ell < z < \frac{1}{4}L. \end{cases} \end{aligned}$$

This theoretically designed waveform is shown in fig. 3, along with that resulting from 3D numerical simulations using CST. **PEAKED PROFILE WITH TWO OSCILLATIONS:** We might also want to generate a peaked profile with many fewer minor oscillations per half-period. However, this cannot be achieved with only slabs of constant ϵ_r . Nevertheless, something closer to the design goal *can* be made if we construct an $\tilde{E}(z)$ using two sinusoidal regions and a quadratic Bezier² function $B(z)$ to interpolate between them. With $\epsilon_r(z)$ from (2), this profile is

$$\tilde{E}(z) = \begin{cases} \lambda_0 \sin(k_0z), & 0 < z < \ell_0 \\ \text{Quadratic-Bezier}, & \ell_0 < z < \ell_1 \\ \lambda_1 \sin(k_1z), & \ell_1 < z < \frac{1}{4}L. \end{cases} \quad (8)$$

For this construction the challenge now becomes that the permittivity becomes very large in a small region; the required ϵ_r can be seen in the inset of fig. 4. Further, even before any difficulties of fabricating an experimental structure are considered, generating numerical results for this is problematic. We can see in fig. 4 the results of using CST to generate a field profile in comparison to the designed-for wave shape – there are significant regions where the match is rather poor. Nevertheless, the general character of the desired wave profile is achieved, and the important high-field peaks *are* closely matched.

Having first considered theoretical structures based on an infinitely periodic representation, we now move to the finite

² See e.g. <http://mathworld.wolfram.com/BezierCurve.html>

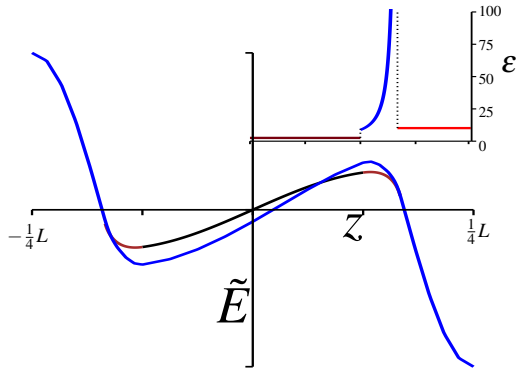


FIG. 4: Field profiles for the the two-oscillations structure. The CST simulated field profile for \tilde{E}_x (blue) is broadly similar but not that well matched to the designed-for profile from (8), with its constant ϵ (black) and quadratic Bezier (red) parts. This is because ϵ_r not only needs to be very large for a very thin slice, but is also rapidly varying. The structure has a $\epsilon(z)$ from (8), with $a_0 = 0.5(\frac{1}{2}L)$, $a_1 = 0.668(\frac{1}{2}L)$, $\lambda_0 = 0.5$, $\lambda_1 = 2.0$, $k_0 = 2.5/(\frac{1}{2}L)$ and $k_2 = 5/(\frac{1}{2}L)$; where the quadratic Bezier, is is given parametrically by $z = (-0.049t^2 + .132t + .25)L$ and $\tilde{E}_z = -.401t^2 + .105t + .474$

structures of the kind most likely to be built. One practical feature of our scheme – the free space field wave profile shaping using a slot – has already been demonstrated. This leaves two important issues: (a) to what extent does the profile shaping persist for a small or finite number of repetitions? (b) will an incident field be transmitted effectively into the structure for modulation? Since the structural periodicity is a good match to the incident wavelength, any device *might* be expected to act more like a Bragg mirror. Consequently, we adapted our CST simulations to treat finite-period structures.

The left hand panel of fig. 5 shows a comparison of the bandstructures for the flat-top wave structure with and without a slot. We can easily see that the character of the bandstructures is preserved and that the slot-induced upward frequency shift is relatively small. This trend was repeated in CST simulations for our other slotted structures.

Since the field profiles and bandstructure do not deteriorate when a slot is present, we can turn to the second question, i.e. whether or not an incident field of the correct/desired operating frequency will be transmitted through the structure and be modulated in the desired way. That we *can* do this is shown by the right hand panel of fig. 5, where we see the reflectivity spectrum for a multiple period structures with and without a slot. As a direct result of our design process, we see that the presence of a slot – and perhaps despite its sub-wavelength

width – enhances transmission into the structure.

In summary, we have demonstrated a considerable freedom to customise electric field profiles, even in free-space, and without resorting to harmonic synthesis. This is achieved by the use of a customised periodic structure with an engineered permittivity profile based on functional materials. The material permittivity function needed can be based either on known solutions, such as specific Mathieu functions, or more generally calculated directly from the wave equation. We have

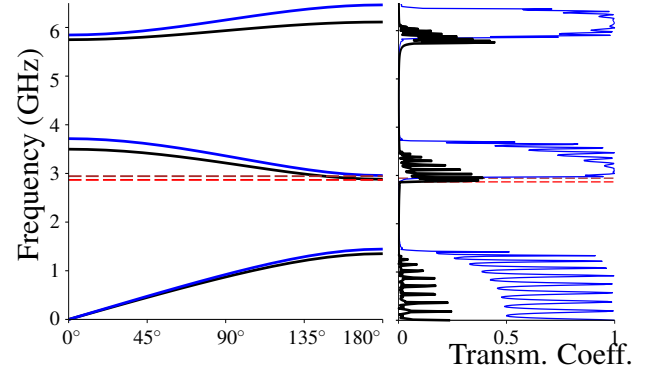


FIG. 5: Bandstructure (left) and transmission coefficients (right) calculated using CST for a 3D ten cell flat-top structure, both without (black) and with (blue) the presence of a slot. The angle gives the phase difference across the length of the unit cell. The operating frequencies (dashed lines) are at a 180° phase shift. Without a slot the frequency is 2.867GHz & 30% transmission (red), and with a slot it is 2.911GHz & 95% (brown). Transmission data was obtained by exciting the structure with a Gaussian pulse of width 52.5ps and time delay 0.1367 ns, and taking results after 60ns of run time.

validated our theoretical conception by implementing sample structures in CST, checked that (i) they generate a field profile that matches the design, (ii) that the profiling can be achieved in free-space by means of a slotted structure, and (iii) that the desired field modes inside the structure can be excited.

In future work we aim to investigate more realistic models of our structures. Further, it seems likely that this scheme can be adapted to other fields such as acoustics.

Acknowledgements

The authors are grateful for the support provided by STFC (the Cockcroft Institute ST/G008248/1) and EPSRC (the Alpha-X project EP/J018171/1 and EP/N028694/1).

[1] J. Gratus, M. McCormack, and R. Letizia, Proceedings of PIERS 2015 in Prague pp. 675–680 (2015).
 [2] J. Gratus, M. McCormack, J. Opt. **17**, 025105 (2015), arXiv:1503.06131, doi:10.1088/2040-8978/17/2/025105.

[3] P. S. J. Russell, T. A. Birks, F. D. Lloyd-Lucas, in *Confined Electrons and Photons: New Physics and Applications*, edited by E. Burstein, C. Weisbuch (1995), vol. 340 of *NATO Advanced Science Institutes Series B*, pp. 585–633.
 [4] P. S. Russell, T. A. Birks, J. Lightwave Techn. **17**, 1982 (1999),

-
- doi:10.1109/50.802984.
- [5] J. D. Joannopoulos, S. G. Johnson, J. N. Winn, R. D. Meade, *Photonic crystals: molding the flow of light* (Princeton, 2011).
- [6] H.-S. Chan, Z.-M. Hsieh, W.-H. Liang, A. H. Kung, C.-K. Lee, C.-J. Lai, R.-P. Pan, L.-H. Peng, *Science* **331**, 1165 (2011), doi:10.1126/science.1198397.
- [7] J. A. Cox, W. P. Putnam, A. Sell, A. Leitenstorfer, F. X. Kärtner, *Opt. Lett.* **37**, 3579 (2012), doi:10.1364/OL.37.003579.
- [8] S. B. P. Radnor, L. E. Chipperfield, P. Kinsler, G. H. C. New, *Phys. Rev. A* **77**, 033806 (2008), arXiv:0803.3597, doi:10.1103/PhysRevA.77.033806.
- [9] P. Piot, Y. E. Sun, J. G. Power, M. Rihaoui, *Phys. Rev. ST Accel. Beams* **14**, 022801 (2011), arXiv:1007.4499, doi:10.1103/PhysRevSTAB.14.022801.
- [10] F. Albert, A. G. R. Thomas, S. P. D. Mangles, S. Banerjee, S. Corde, A. Flacco, M. Litos, D. Neely, J. Vieira, Z. Najmudin, *Plasma Physics and Controlled Fusion* **56**, 084015 (2014), doi:10.1088/0741-3335/56/8/084015.
- [11] CST AG, Germany, *CST Studio Suite*, <http://www.cst.com/>.
- [12] A. El Haddad, *Optik* **127**, 1627 (2016), doi:10.1016/j.ijleo.2015.11.049.
- [13] J. Gratus, P. Kinsler, R. Letizia, T. Boyd, in *Proceedings of META16 Malaga - Spain. The 7th International Conference on Metamaterials, Photonic Crystals and Plasmonics* (2016), in review.
- [14] M. C. Kohler, T. Pfeifer, K. Z. Hatsagortsyan, C. H. Keitel, in *Advances In Atomic Molecular and Optical Physics, Volume 61*, edited by E. Arimondo, P. R. Berman, and C. C. Lin (Elsevier, 2012), vol. 61 of *Advances In Atomic Molecular and Optical Physics*, pp. 159–207, doi:10.1016/B978-0-12-396482-3.00004-1.